



HAL
open science

Antiproliferative in Vitro Evaluation of Terpenic Amines Synthesized via a Rhodium-catalyzed Hydroaminomethylation

Alejandro Perez Alonso, Laure Gibot, Isabelle Favier, Doan Pham Minh,
Montserrat Gómez, Daniel Pla

► To cite this version:

Alejandro Perez Alonso, Laure Gibot, Isabelle Favier, Doan Pham Minh, Montserrat Gómez, et al..
Antiproliferative in Vitro Evaluation of Terpenic Amines Synthesized via a Rhodium-catalyzed Hydroaminomethylation. *Chemistry and Biodiversity*, 2024, pp.e202301431. 10.1002/cbdv.202301431 .
hal-04464878

HAL Id: hal-04464878

<https://imt-mines-albi.hal.science/hal-04464878v1>

Submitted on 20 Feb 2024

HAL is a multi-disciplinary open access archive for the deposit and dissemination of scientific research documents, whether they are published or not. The documents may come from teaching and research institutions in France or abroad, or from public or private research centers.

L'archive ouverte pluridisciplinaire **HAL**, est destinée au dépôt et à la diffusion de documents scientifiques de niveau recherche, publiés ou non, émanant des établissements d'enseignement et de recherche français ou étrangers, des laboratoires publics ou privés.

Antiproliferative *in Vitro* Evaluation of Terpenic Amines Synthesized via a Rhodium-catalyzed Hydroaminomethylation

Alejandro Pérez Alonso,^[a] Laure Gibot,^[b] Isabelle Favier,^[a] Doan Pham Minh,^[c] Montserrat Gómez,^[a] and Daniel Pla,^[a]

[a] Dr. A. Pérez Alonso, Prof. M. Gómez, Dr. D. Pla,
Laboratoire Hétérochimie Fondamentale et Appliquée, UMR CNRS 5069
Université Toulouse III – Paul Sabatier
118 route de Narbonne, 31062 Toulouse Cedex 9, France
E-mail: montserrat.gomez-simon@univ-tlse3.fr; pla@lhfa.fr

[b] Dr. L. Gibot
Laboratoire des IMRCP, Université de Toulouse, CNRS UMR 5623
Université Toulouse III – Paul Sabatier
118 route de Narbonne, 31062 Toulouse Cedex 9, France

[c] Prof. D. Pham Minh
Centre RAPSODEE
Université de Toulouse, IMT Mines Albi, UMR CNRS 5302
Campus Jarlard, 81013 Albi Cedex 9, France

Abstract: Terpene-derived alkaloids show a variety of biological activities, including antioxidant, anti-inflammatory, antimicrobial and cytotoxicity effects. In this work, homologated monoterpene amines have been prepared via a rhodium-catalyzed hydroaminomethylation of biomass-based alkenes, such as (*R*)-limonene, linalool, myrcene and camphene, in combination with secondary amines of aliphatic and aromatic nature, namely morpholine and *N*-methylaniline, leading to highly chemo- and regioselective processes. The as-prepared amines were obtained in 50-99% overall yields, and *in vitro* tested on a human colon cancer cell line (HCT-116) to evaluate their cytotoxic potential. The lead compound of the series (**3a**) showed cytotoxicity in the micromolar range (IC₅₀ 52.46 μ M) via the induction of cell death by apoptosis, paving the way towards further structure-activity relationship studies.

Introduction

The monoterpene alkaloids, a group of compounds consisting of two isoprene units that contain one or more nitrogen atoms in their structure, has yielded a large number of biologically active compounds presenting cytotoxic activity (Figure 1).^[1] Specifically, *N*-myrtenyl-1-adamantylamine exhibited high activity against CEM-13, MT-4, and U-937 human leukemia cell lines^[2] via tyrosyl-DNA phosphodiesterase inhibition,^[3] as well as related peptide conjugates against human gastric adenocarcinoma (AGS), human breast adenocarcinoma (MCF-7) and human colon adenocarcinoma (HT-29) proliferation in the low nanomolar range.^[4] Furthermore, a structurally related 1-adamantanecarboxamides containing pinene,^[2] myrtenyl and citronellyl moieties^[5] showed both promising cytotoxicity and inhibitory activity against orthopoxviruses. More complex structures featuring citronellyl^[6]

and isopinocampheyl^[7] monoterpene moieties showed anti-influenza and antimycobacterial activities, respectively.

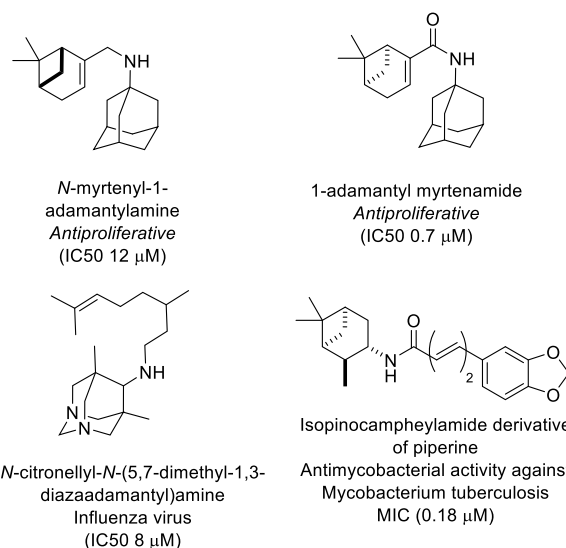


Figure 1. Synthetic monoterpene alkaloids exhibiting broad biological activities: antiproliferative, antibiotic and antiviral in the low micromolar range.

Inspired by the broad range of biological activities of terpenic alkaloids, this study aims at the synthesis and cytotoxicity evaluation of homologated derivatives. In particular, hydroaminomethylation (HAM) represents a highly atom-economic strategy that enables not only terpene homologation but also the introduction of nitrogenated functions on enantiopure renewable feedstocks of relevance, providing efficient multi-component tandem processes. A few literature reports have

described the HAM of limonene, camphene and β -pinene, using rhodium-based catalysis (0.1-1 mol% catalyst loadings) and 1:1 mixtures of syngas at high pressures (40-80 bar) in non-protic organic solvents such as PhMe, MeCN or THF at temperatures ranging from 80 to 120 °C to yield the desired amine products, albeit in moderate yields and low selectivity.^[8]

Strategies facilitating the completion of HAM tandem process, and most notably providing efficient means to facilitate the final enamine reduction via multimetallic catalytic systems,^[9] or the use of glycerol as hydrogen transfer booster,^[10] as proven by our group, represent promising means for the transformation of recalcitrant substrates. Thus, terpene homologation via HAM prompted us to explore the chemical space^[11] around naturally occurring monoterpenes via green diversity-oriented synthesis strategies in glycerol,^[12] solvent that permits both to immobilize efficiently the metal-based species and to enhance the reaction by promoting the reduction of the enamine intermediate.^[10] In this regard, the direct functionalization of unactivated terpenes represents a powerful and sustainable strategy in synthesis, enabling new entries for translational science in drug discovery provided that selective transformations can be implemented.

Results and Discussion

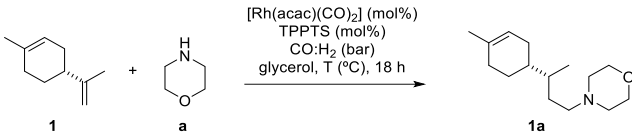
Chemistry

Given the sterical hindrance of terpenes in comparison to other unactivated alkenes in particular terminal alkyl-based alkenes, (*R*)-limonene (**1**) and morpholine (**a**) were chosen as benchmark reactants for the optimization of the HAM reaction conditions (Table 1). Our study started by examining previously used conditions for terminal alkyl alkenes and styrene derivatives in neat glycerol,^[10] acting both as an alternative solvent and reducing agent in the HAM of oct-1-ene [120 °C, 6 h, 10 bar total pressure, and 1 mol% [Rh(acac)(CO)₂] and 2 mol% TPPTS (trisodium 3,3',3''-phosphanetriyltri(benzene-1-sulfonate) loadings], but these conditions did not work when the terpenic substrate was used (entry 1, Table 1). Although increasing the reaction time to 18 h failed to give **1a** (entry 2, Table 1), we found that higher reaction pressures (20 and 40 bar total pressure of a 1:1 mixture of H₂ and CO) enabled the HAM reaction, albeit with moderate yields (entries 3-5, Table 1). The strong influence of operating at high pressure of syngas should be noted (H₂ and CO 1:1 binary mixtures, 40 bar total pressure, entry 4, Table 1), and not the total pressure of the system (at least under the conditions studied) as neither a gas mixture of 1:1:2 of H₂, CO and N₂ at 40 bar (entry 5, Table 1), nor the reaction conducted at a lower pressure of a 1:1 mixture of H₂ and CO (20 bar total pressure, entry 3, Table 1) afforded good yields (10 and 15% yield, respectively). In this transformation, both the Rh organometallic precursor and the ligand TPPTS play essential roles, as evidenced in the lack of conversion obtained for reaction controls (in the absence of the former and the latter, respectively; entries 6-7, Table 1). To improve the yield of the reaction, we surveyed higher catalyst loadings. Using 2 and 5 mol% of rhodium catalyst, almost quantitative yields were obtained (95% and 99% yields, respectively; entries 8-9, Table 1). Furthermore, we studied the effect of the temperature (entries 10-11, Table 1), but no improvement was achieved at lower reaction temperatures, obtaining only a 77% yield at 60 °C; no reaction conversion took place at room temperature, probably due to the high viscosity of glycerol (entries 10-11, Table 1). Taking these results into account, the following optimized conditions were

selected for the reaction scope study: 2 mol% [Rh(acac)(CO)₂], 4 mol% TPPTS, 120 °C, 18 h and a 1:1 mixture of H₂ and CO at 40 bar of total pressure in neat glycerol (entry 8, Table 1), which led exclusively the linear regioisomer.

With the optimized reaction conditions in hand, we next investigated the substrate scope with three additional monoterpenes, namely linalool (**2**), myrcene (**3**), and camphene (**4**) in combination with two amines: morpholine (**a**) and *N*-methylaniline (**b**) (Scheme 1). Notably, the reaction regioselectivity was impacted by the amine used. Whereas the use of morpholine (**a**) afforded exclusively linear amine products (**1a**, **2a**, **3a**, **4a**), *N*-methylaniline (**b**) also gave low amounts of the branched regioisomer [for **1b**, **2b**, **3b** and **4b**, 91:9 to 80:20 ratios for linear to branched (*l/b*)] (Scheme 1).

Table 1. Optimization of Rh-catalyzed hydroaminomethylation involving (*R*)-limonene and morpholine as reactants.



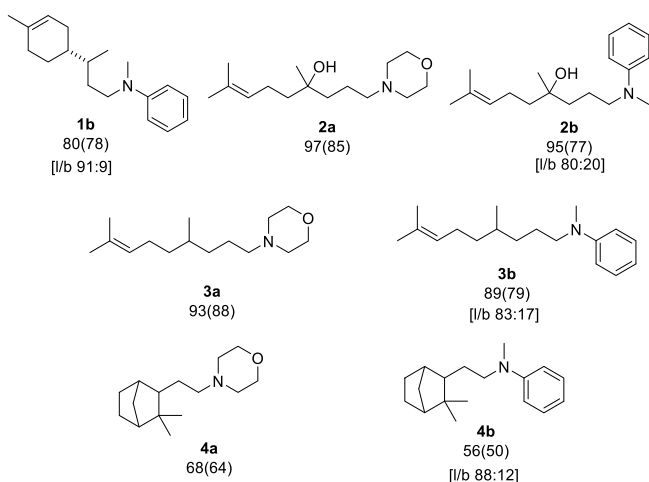
Entry	[Rh] (mol%)	TPPTS (mol%)	P _{H₂} :P _{CO} (bar)	T (°C)	Conv. (%) ^b	Yield (%) ^b
1 ^c	1	2	5:5	120	0	-
2	1	2	5:5	120	0	-
3	1	2	10:10	120	18	15
4	1	2	20:20	120	60	50
5 ^d	1	2	10:10	120	12	10
6	0	2	20:20	120	0	-
7	1	0	20:20	120	0	-
8	2	4	20:20	120	97	95
9	5	10	20:20	120	99	99
10	2	4	20:20	25	>5	>5
11	2	4	20:20	60	77	76

^a Results from duplicate experiments. Reaction conditions: 1 mmol of (*R*)-limonene, 1.5 mmol of morpholine and 2 mL of glycerol. ^b Determined by GC-FID using 1,3,5-tribromobenzene as internal standard. ^c Reaction time: 6 h. ^d Gas mixture: H₂/CO/N₂ = 10:10:20.

As a general trend, both series of homologated terpene amines were successfully synthesized via a Rh-catalyzed HAM reaction in 50-95% yields (Scheme 1). Morpholine led to higher product yields in comparison to *N*-methylaniline, probably due to the lower nucleophilicity of the latter. In particular, for linalool and myrcene, HAM proceeded exclusively at the monosubstituted C=C bond under the optimized reaction conditions, leading to **2a**, **2b**, **3a** and **3b** in good to high yields (79-88%). For myrcene amines (**3a**, **3b**), it is important to mention that the hydrogenation of the C=C geminal bond occurred selectively under the optimized HAM reaction conditions, with no reduction of the trisubstituted prenyl group. It is worth to mention that the high selectivity

of the monometallic Rh system described herein for substrates **2** and **3** in terms of hydroformylation selectivity (for **3**), as well as precluding undesired hydrogenation of mono-substituted alkene moieties (for both **2** and **3**), could not be achieved with a more active Rh/Co catalytic systems previously reported by our group.^[12]

The geminal alkene present in camphene was less reactive towards HAM than the other monoterpenes tested probably due to its sterical hindrance, but the homologated derivatives of camphene with morpholine (**4a**) and aniline (**4b**) were obtained in 64 and 50% yield, respectively. Slightly better yields of 71 and 58% for **4a** and **4b**, respectively, were obtained using a Rh/Co bimetallic catalytic system.^[12] After purification via flash column chromatography, the as-prepared products were then subjected to biological evaluation to assess their antiproliferative effects on human tumor cells as follows.



Scheme 1. Hydroaminomethylation reaction scope. Reaction conditions: 1 mmol of terpene, 1.5 mmol of amine, 20 bar H₂, 20 bar CO, 0.02 mmol [Rh(acac)(CO)₂], 0.04 mmol TPPTS, and 2 mL of glycerol at 120 °C for 18 h. Conversions and yields (in brackets) were determined by GC-FID, using 1,3,5-tribromobenzene as internal standard. For **1a**, see Table 1.

Biological Evaluation

The as-prepared compounds presented *in vitro* antitumor properties via distinct cell mechanisms, namely anti-proliferative or pro-apoptotic effects. The antitumor potential of these terpenic amines was tested *in vitro* on human colorectal cancer cells (HCT-116). Videomicroscopy was used to monitor the growth of cells exposed to increasing concentrations of compounds in the range 0.39 μ M to 100 μ M over 72 h (Figure 2). Despite the fact that all compounds prevented cell growth at 100 μ M concentration, their magnitudes were different. Indeed, it could be noted that the behavior of compounds **3a** and **4b** induced a total arrest of cell growth, while all other compounds slowed down cell growth. Although the experimental data is not precise enough to conclude on the half maximal inhibitory concentration (IC₅₀) of these compounds, they appear to be in the 50-100 μ M range for them all.

For the subsequent experiments, the most effective concentration, *i.e.* 100 μ M, was used to treat the cells in order to determine the antitumor mechanisms of the different compounds (Figure 3). The strategy was to simultaneously quantify cell proliferation using a fluorescent probe that labels nuclei in red while quantifying cell death by apoptosis, the most common programmed cell death, using a probe which fluoresces in green when Caspases 3 and 7 were activated due to apoptosis

induction. Videomicroscopy was also used to quantify the number of cells, *i.e.* cell proliferation, during the 72 h of exposure to 100 μ M of the different compounds (Figure 3A). It clearly appeared that compounds **3a** and **4b** totally inhibit proliferation, as had been observed with the monitoring of cell growth by measuring cell confluence. In these cases, cell proliferation was similar to the positive control 1 μ M staurosporine, known as a potent pro-apoptotic inducer.^[13] The other compounds (**1a**, **2a**, **1b**, **2b** and **3b**) decreased cell proliferation but did not stop it. In parallel, cell death by apoptosis was followed in a kinetic manner (Figure 3B). Interestingly, compounds **1b**, **3a** and **4b** induced apoptosis over the time. Representative pictures of the different conditions after 48 h of incubation with the different compounds are shown in Figure 3C. Cells dying by apoptosis pathway were labelled in green while all the nuclei of the cells were labelled in red. The quantification of cell nuclei per image 48 h post-treatment indicated that all the compounds led to a statistically significant decrease in cell proliferation, more pronounced for **1b**, **3a** and **4b** with similar number of cells than in positive control condition treated with cell death inducer staurosporine (Figure 3D). Interestingly, the quantification of cell death by apoptosis 48 h post-treatment indicated that these three compounds led to a statistically significant induction of apoptosis, similar to the positive control treated with apoptosis-inducer staurosporine. These two complementary types of experiments allowed to conclude that compounds **1b**, **3a** and **4b** displayed an anti-tumor effect by inducing a cell death mechanism by apoptosis. On the other hand, all the other compounds (**1a**, **2a**, **2b**, **3b** and **4a**) showed an anti-tumor effect which was mainly due to an inhibition of cell proliferation and not to the induction of cell death by apoptosis. Indeed, for these amines, the normal appearance of the cell morphology over time and the absence of detached cells suggest a blockage of cell proliferation mechanism rather than for the induction of cell death other than apoptosis (*e.g.* necrosis, autophagy, pyroptosis).^[14]

Experimental

General Material and Methods

Unless otherwise stated, chemical reactants and reagents were obtained from commercial suppliers and used without further purification. Glycerol was dried under vacuum at 80 °C for 18 h prior to use. NMR spectra were recorded on a Bruker Avance 300 spectrometer at 293 K (300 MHz for ¹H NMR and 75.4 MHz for ¹³C NMR). Chemical shifts (δ) are reported in ppm referenced to the appropriate residual deuterated solvent peaks; coupling constants are reported in Hz. The multiplicity of signals is indicated using the following abbreviations: s = singlet, d = doublet, t = triplet, q = quadruplet, bs = broad singlet, bd = broad doublet, m = multiplet. GC-MS analyses were performed on a GC Perkin Elmer Clarus 500 with a flame ionization detector (FID) using a SGE BPX5 column (30 m x 0.32 mm x 0.25 mm) composed of 5% phenylmethylsiloxane and a Perkin Elmer Clarus 560 S mass spectrometer. The injector temperature was 250 °C and the flow was 2 mL/min. The temperature program was 45 °C for 2 min, 20 °C/min to 300 °C, hold for 5 min.

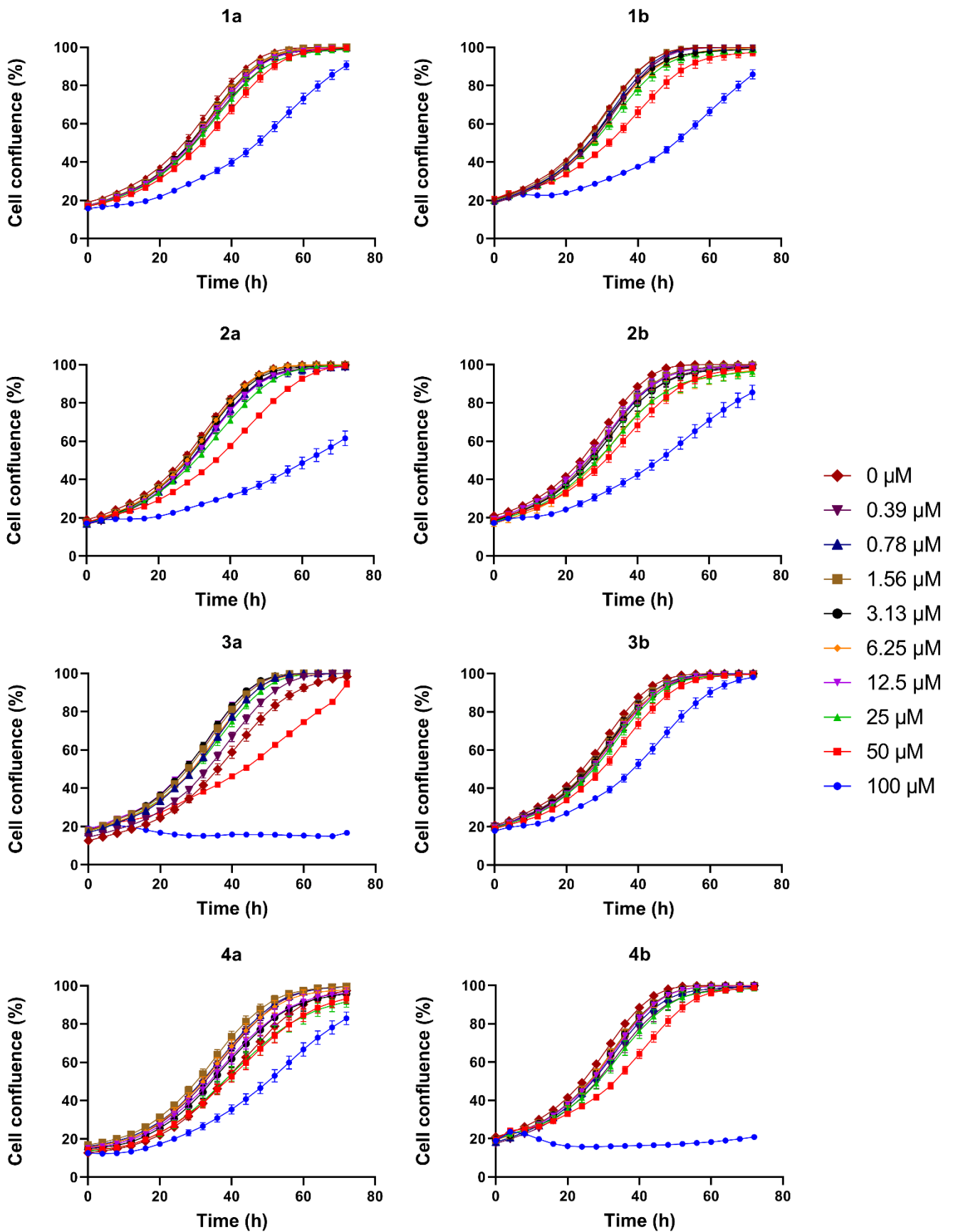


Figure 2. Kinetic monitoring of the viability of human colon cancer cells (HCT-116) exposed to increasing concentrations of compounds from 0 μM to 100 μM. Cell growth was observed in real-time by videomicroscopy over 72 h. Data (mean ± SEM) represent 2 independent experiments, with a total of 9 biological replicates.

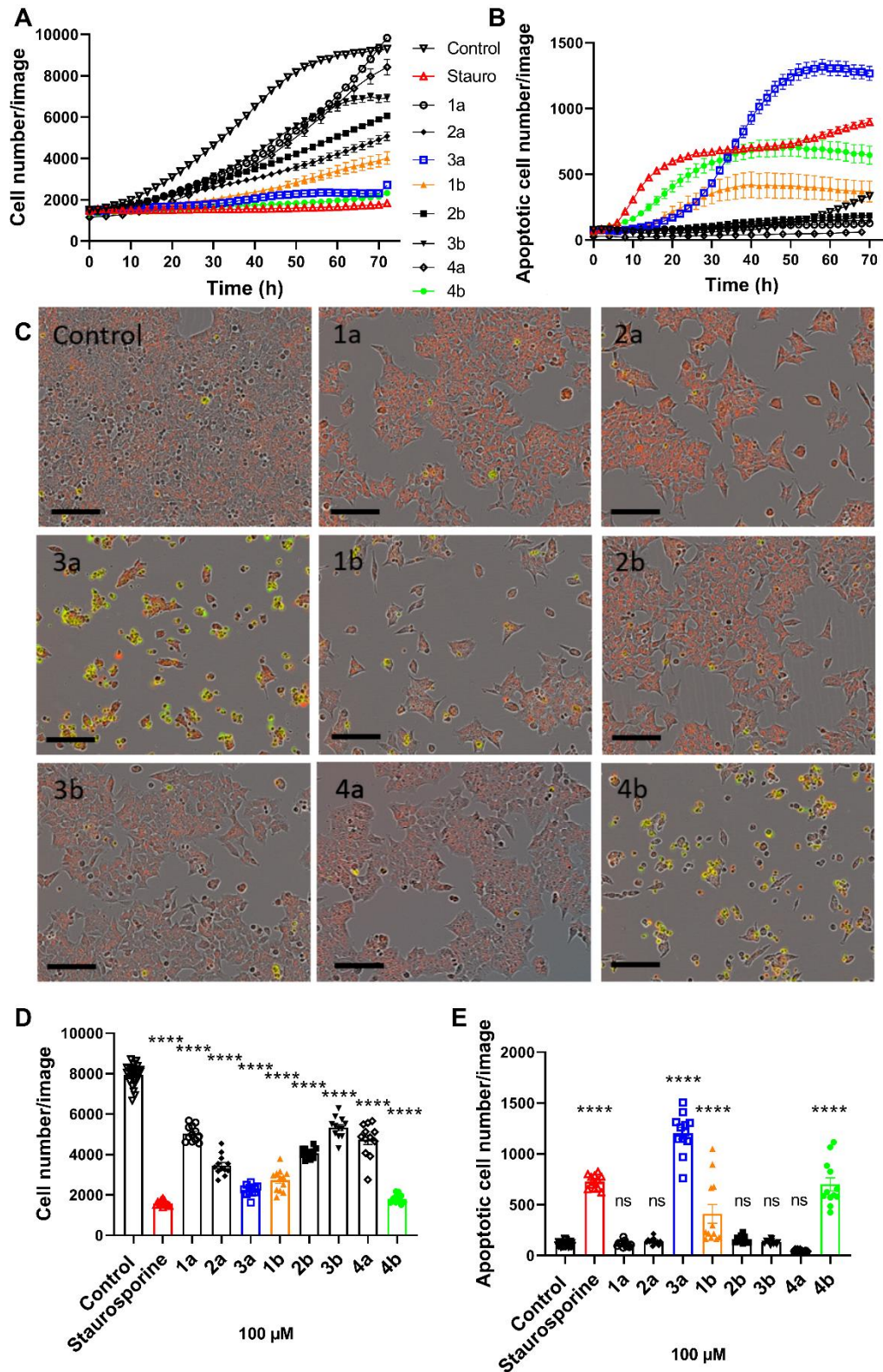
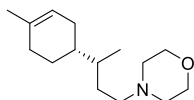


Figure 3. Quantification of cell proliferation and cell death by apoptosis induced by the different compounds at 100 μ M. A) Kinetic monitoring of HCT-116 cell number (proliferation) exposed to 100 μ M of the different compounds over 72 h by videomicroscopy. B) Kinetic monitoring of HCT-116 cell death by apoptosis when exposed to 100 μ M of the different compounds over 72 h by videomicroscopy. C) Representative pictures showing in phase the cell appearance and confluence, in red the nuclei of all cells and in green the cells undergoing the mechanism of cell death by apoptosis, after 48 h of treatment with the different compounds. Scale bar: 100 μ m. D) Quantification of cell proliferation after 48 h of incubation with the different compounds at 100 μ M, using nuclei labelling with NuLight red fluorescent probe. E) Quantification of the number of cells undergoing cell death by apoptosis after 48 h of incubation with the different compounds at 100 μ M, using Caspase-3/7 green fluorescent dye. Staurosporine (Stauro) (1 μ M) was used as a positive control for induction of apoptosis. Data (mean \pm SEM) represent a total of 6 biological replicates. Data have been statistically analyzed using one-way ANOVA followed by Dunnett's post-test to compare every condition to the control one (untreated cells).

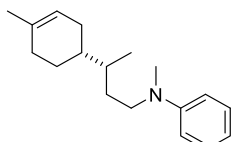
Synthesis of Terpene Amines

The terpene (1.0 mmol) and the corresponding amine (1.5 mmol) were dissolved in 2 mL of dried glycerol in the presence of the appropriate amount of [Rh(acac)(CO)₂] (from 1 to 5 mol% of Rh) and TPPTS. Once the autoclave was sealed, it was pressurized at the working pressure and the reactor was heated up to 120 °C. After depressurization and cooling down to room temperature, the glycerol was extracted with CH₂Cl₂ (3 x 4 mL) and the combined organic extracts were filtered through Celite. The combined organic fractions were analyzed by Gas Chromatography coupled with a Mass Spectrometry and FID detectors, using 1,3,5-tribromobenzene as internal standard, unless otherwise stated.

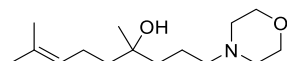
Characterization Data of Terpene Amines



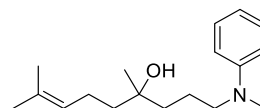
4-((*S*)-3-((*R*)-4-methylcyclohex-3-en-1-yl)butyl)morpholine (**1a**). Diastereomeric mixture, characterization data matches literature reports.^[8a, 15] **¹H NMR (300 MHz, CDCl₃)** δ 5.43 – 5.32 (m, 1H), 3.78 – 3.64 (m, 4H), 2.51 – 2.41 (m, 4H), 2.41 – 2.27 (m, 2H), 1.95 (dt, *J* = 5.4, 2.1 Hz, 4H), 1.72 – 1.58 (m, 4H), 1.46 – 1.21 (m, 6H), 0.88 (dd, *J* = 6.3, 3.7 Hz, 4H). **¹³C NMR (75 MHz, CDCl₃)** δ 134.0, 121.0, 120.9, 67.0, 57.7, 53.9, 45.8, 40.6, 38.7, 38.5, 35.8, 35.6, 31.0, 30.9, 30.6, 29.3, 27.6, 27.0, 25.5, 23.5, 16.5, 16.1. **HRMS (DCI-CH₄)** [M+H]⁺ calculated for m/z C₁₅H₂₈NO 238.2171 found 238.2167.



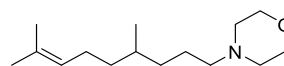
N-Methyl-*N*-((*S*)-3-((*R*)-4-methylcyclohex-3-en-1-yl)butyl)aniline (**1b**). Diastereomeric mixture, characterization data matches literature reports.^[16] **¹H NMR (300 MHz, CDCl₃)** δ 7.34 – 7.18 (m, 2H), 6.87 – 6.61 (m, 3H), 5.51 – 5.37 (m, 1H), 3.59 – 3.20 (m, 2H), 2.96 (s, 3H), 2.19 – 1.92 (m, 4H), 1.69 (s, 3H), 1.51 – 1.25 (m, 5H), 1.07 – 0.91 (m, 4H). **¹³C NMR (75 MHz, CDCl₃)** δ 149.4, 134.1, 129.3, 121.0, 116.0, 112.2, 51.4, 38.9, 38.6, 38.2, 35.5, 35.3, 31.0, 30.6, 30.3, 29.5, 27.8, 27.1, 25.6, 23.6, 16.5, 16.1. **HRMS (DCI-CH₄)** [M+H]⁺ calculated for m/z C₁₈H₂₈N 258.2222 found 258.2215.



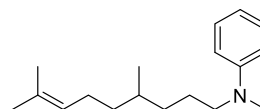
4,8-Dimethyl-1-(morpholin-4-yl)non-7-en-4-ol (**2a**). **¹H NMR (300 MHz, CDCl₃)** δ 5.10 (ddq, *J* = 8.5, 5.7, 1.4 Hz, 1H), 3.71 (t, *J* = 4.7 Hz, 4H), 2.54 – 2.43 (m, 4H), 2.37 (t, *J* = 5.5 Hz, 2H), 2.07 – 1.94 (m, 2H), 1.67 (s, 3H), 1.60 (s, 3H), 1.51 – 1.21 (m, 4H), 1.14 (s, 3H), 0.99 – 0.75 (m, 2H). **¹³C NMR (75 MHz, CDCl₃)** δ 131.5, 124.9, 71.0, 66.7, 59.9, 53.8, 42.5, 41.2, 27.2, 25.9, 23.2, 20.8, 17.8. **HRMS (DCI-CH₄)** [M+H]⁺ calculated for C₁₅H₃₀NO₂ 256.2277 found 256.2278.



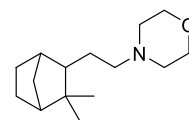
4,8-Dimethyl-1-[methyl(phenyl)amino]non-7-en-4-ol (**2b**). **¹H NMR (300 MHz, CDCl₃)** δ 7.26 – 7.09 (m, 2H), 6.79 – 6.65 (m, 3H), 5.12 (tdd, *J* = 5.7, 2.9, 1.4 Hz, 1H), 3.31 (t, *J* = 7.3 Hz, 2H), 2.93 (s, 3H), 2.02 (dd, *J* = 10.4, 6.2 Hz, 2H), 1.69 (d, *J* = 1.3 Hz, 3H), 1.68 – 1.57 (m, 5H), 1.54 – 1.41 (m, 4H), 1.18 (s, 3H). **¹³C NMR (75 MHz, CDCl₃)** δ 149.5, 132.0, 129.3, 124.5, 116.3, 112.5, 72.8, 53.4, 41.8, 39.3, 38.5, 27.0, 25.8, 22.8, 21.4, 17.8. **HRMS (DCI-CH₄)** [M+H]⁺ calculated for m/z C₁₈H₃₀NO 276.2327 found 276.2328.



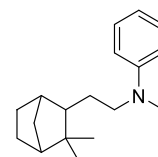
4-(4,8-Dimethylnon-7-en-1-yl)morpholine (**3a**). **¹H NMR (300 MHz, CDCl₃)** δ 5.04 (tp, *J* = 7.1, 1.4 Hz, 1H), 3.66 (t, *J* = 4.7 Hz, 4H), 2.41 (t, *J* = 4.5 Hz, 4H), 2.29 (ddd, *J* = 9.8, 5.9, 3.5 Hz, 2H), 1.92 (dt, *J* = 14.3, 6.9 Hz, 2H), 1.63 (d, *J* = 1.2 Hz, 3H), 1.55 (s, 3H), 1.53 – 1.04 (m, 7H), 0.85 (d, *J* = 6.5 Hz, 3H). **¹³C NMR (75 MHz, CDCl₃)** δ 131.1, 124.8, 67.1, 57.3, 54.0, 37.3, 33.6, 31.1, 25.8, 25.5, 19.8, 17.7. **HRMS (DCI-CH₄)** [M+H]⁺ calculated for m/z C₁₅H₃₀NO 240.2327 found 240.2321.



N-(4,8-Dimethylnon-7-en-1-yl)-*N*-methylaniline (**3b**). **¹H NMR (300 MHz, CDCl₃)** δ 7.29 – 7.20 (m, 2H), 6.77 – 6.65 (m, 3H), 5.12 (ddt, *J* = 7.1, 5.7, 1.5 Hz, 1H), 3.35 (ddd, *J* = 9.3, 8.3, 5.5 Hz, 2H), 2.93 (s, 3H), 2.12 – 1.90 (m, 2H), 1.71 (d, *J* = 1.4 Hz, 3H), 1.63 (d, *J* = 1.4 Hz, 3H), 1.59 – 1.14 (m, 7H), 0.97 (d, *J* = 6.3 Hz, 3H). **¹³C NMR (75 MHz, CDCl₃)** δ 149.5, 131.4, 129.3, 124.8, 116.0, 112.3, 51.0, 38.2, 37.2, 33.3, 30.7, 25.9, 25.6, 19.8, 17.8. **HRMS (DCI-CH₄)** [M+H]⁺ calculated for C₁₈H₃₀N 260.2378 found 260.2380.



4-[2-(3,3-Dimethylbicyclo[2.2.1]heptan-2-yl)ethyl]morpholine (**4a**). Diastereomeric mixture in a (6:4) ratio, characterization data matches literature reports.^[12] **¹H NMR (300 MHz, CD₃CN)** δ 3.59 (t, *J* = 4.8 Hz, 4H), 2.36 (t, *J* = 4.3 Hz, 4H), 2.23 – 2.17 (m, 2H), 2.10 (bs, 1H), 1.74 – 1.06 (m, 8H), 0.96 and 0.93 (2s, 3H), 0.89 and 0.82 (2s, 3H). **¹³C NMR (75 MHz, CD₃CN)** δ 67.6, 60.1, 59.6, 54.8, 53.3, 50.3, 50.0, 49.2, 43.9, 42.1, 41.2, 37.7, 37.6, 36.4, 32.7, 30.6, 28.5, 28.2, 25.3, 25.1, 24.8, 24.1, 21.8, 20.6. **HRMS (DCI-CH₄)** [M+H]⁺ calculated for m/z C₁₅H₂₈NO 238.2171 found 238.2162.



N-[2-(3,3-Dimethylbicyclo[2.2.1]heptan-2-yl)ethyl]-*N*-methylaniline (**4b**). **¹H NMR (300 MHz, CDCl₃)** δ 7.34 – 7.15 (m, 3H), 6.80 – 6.68 (m, 2H), 3.47 – 3.11 (m, 2H), 2.97 (d, *J* = 1.6 Hz, 3H), 2.22 (t, *J* = 2.9 Hz, 1H), 2.06 (dd, *J* = 4.4, 1.6 Hz, 1H), 1.83 – 1.49 (m, 6H), 1.45 – 1.10 (m, 5H), 1.03 (s, 3H), 1.01 (s, 3H), 0.93 (s, 3H), 0.86 (s, 3H). **¹³C**

NMR (75 MHz, CDCl₃) δ 129.2, 117.3, 115.8 (2s), 112.1, 112.0, 53.2, 52.8, 52.2, 49.2, 48.9, 48.4, 42.8, 41.0, 38.2 (2s), 37.1, 36.0, 32.5, 30.0, 28.0, 27.3, 24.9, 24.7, 24.1, 23.0, 21.6, 20.1. **HRMS (DCI-CH₄)** [M+H]⁺ calculated for m/z C₁₈H₂₈N 258.2222 found 258.2219.

Cytotoxicity Experiments

Cell culture. Human HCT-116 colorectal cancer cells (CCL-247) were purchased from ATCC at passage 0 (P0) and used under passage 6. Cells were grown in Dulbecco's Modified Eagle Medium (DMEM) containing 4.5 g/L glucose, GLUTAMax and pyruvate, supplemented with 10% of heat-inactivated fetal bovine serum and 100 U/ml penicillin, and 100 μ g/ml streptomycin. Cells were maintained at 37 °C in a humidified atmosphere containing 5% CO₂. Cell culture media were changed three times a week. Cells were tested negative for mycoplasma using MycoAlert mycoplasma detection kit (Lonza) all along the experiments.

Cell growth measurement. The day prior the experiment, 10,000 HCT-116 cells were plated in 96-well plates, which represents approximately a 20% of confluence. This seeding density was chosen in order to allow cell proliferation to occur over several days. The day of the experiment, cells were treated with 9 two-fold serial dilutions of the homologated terpene amines in 200 μ L of cell culture medium, from 100 μ M to 0.39 μ M. Plates were then placed in a videomicroscope Incucyte S3 (Sartorius) and pictures were taken at 10x every 4 h for 72 h and analyzed with the Incucyte-associated software. Cell viability was determined as area occupied by the cells (confluence) over the time. Two independent experiments with 3 and then 6 independent biological replicates respectively were led.

Cell proliferation and apoptosis quantification. As mentioned above, 10,000 HCT-116 cells were plated the day before the experiment in 96-well plates. Cell proliferation and cell apoptosis were quantified simultaneously in the well by videomicroscopy using specific fluorescent markers. NuLight Rapid red dye (Sartorius) (1/2000) and Caspase-3/7 dye (Sartorius) (1/2000) were diluted in cell culture medium together with either 50 μ M or 100 μ M of the homologated terpene amines. NuLight red dye aims at labelling nuclei of live cells while Caspase-3/7 dye becomes fluorescent (green) when cell death apoptosis mechanism is active. Plates were then placed in a videomicroscope Incucyte S3 (Sartorius) and pictures (phase, green and red fluorescence) were taken at 10x every 1 h for 72 h and analyzed with the Incucyte-associated software. One experiment was led with 6 biological replicates; two pictures being taken per well. Incubation with 1 μ M staurosporine was used as positive control for apoptosis induction.

Statistical analysis. Data analysis was performed using GraphPad Prism 8 Software (La Jolla, CA, USA) and independent biological replicates data were plotted and expressed as mean \pm standard error to the mean (SEM). Data have been statistically analysed using one-way ANOVA followed either by Dunnett's post-test to compare every condition (compounds) to the control one (untreated cells). ns: non-significant, * p <0.05, ** p <0.01, *** p <0.001 and **** p <0.0001.

Conclusion

An efficient rhodium-catalyzed HAM methodology in glycerol was applied to the diverted synthesis of homologated terpene amines in good to excellent yields. This tandem strategy allowed the preparation of novel alkaloids with untapped biological potential through straightforward installation of nitrogenated motifs on naturally occurring monoterpene substrates via a catalytic multi-component strategy leading to highly chemo- and regio-selective processes.

The anti-proliferative activity of the as-prepared compounds was assessed *in vitro* on human colorectal cancer cells (HCT-116), showing either a partial cell growth inhibition for **1a**, **2a**, **1b**, **2b** and **3b**, or a complete proliferation inhibition for **3a** and **4b** in the micromolar range. Apoptotic cell death via the activation of caspases 3/7 was detected for **1b**, **3a** and **4b**, evidencing distinct cell mechanisms. Being **3a** the most potent compound of the series, a half-maximal inhibitory concentration (IC₅₀) of 52.46 μ M could be determined (see Figure S11 in the Supp. Info), which is in the micromolar range as the parent myrcene compound (**3**, IC₅₀ = 9.32 μ M).^[17] The weak cytotoxicity activity exhibited by the other compounds of the series opens new avenues towards their assessment as novel biomass-derived compounds to be screened against applications of societal relevance with safe cytotoxicity profiles (e.g. multidrug-resistant bacterial or fungal infections). On the basis of this work, the paramount importance of chemical space bio-prospection on natural sources and further structure-activity relationship studies is instrumental to find new lead candidates in drug discovery.

Supporting Information

¹H, ¹³C and 2D NMR spectra and high-resolution MS data of terpene amines are reported as Supporting Information in PDF.

Acknowledgements

Authors thank the Université Toulouse III – Paul Sabatier, IMT Mines Albi and the Centre National de la Recherche Scientifique (CNRS) for their financial support. A. P. A. thanks the Université Fédérale de Toulouse and the Occitanie Region for his doctoral fellowship (APR2019-CATPROC). We would like to thank the Institut de Chimie de Toulouse ICT – UAR 2599 (Université de Toulouse, CNRS, Toulouse, France – www.ict.cnrs.fr) for its participation in the purchase of the videomicroscope used in this study.

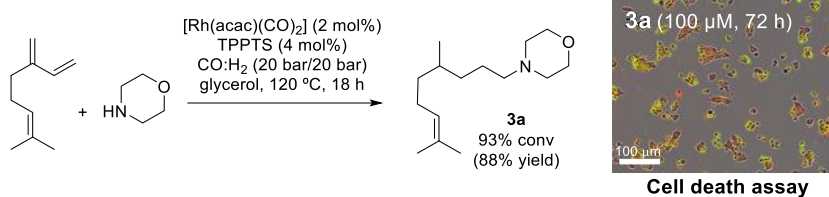
Keywords: hydroaminomethylation • multi-component tandem processes • biomass-based amines • growth inhibition • apoptosis

[1] a) H. Kikuchi, T. Nishimura, E. Kwon, J. Kawai, Y. Oshima, *Chem. Eur. J.* **2016**, *22*, 15819; b) M. Zhang, Y. Wang, S. Wang, H. Wu, *Molecules* **2022**, *27*, 8104; c) M. Zielińska-Błajet, J. Feder-Kubis, *Int. J. Mol. Sci.* **2020**, *21*, 7078.

[2] E. V. Suslov, K. Yu. Ponomarev, A. D. Rogachev, M. A. Pokrovsky, A. G. Pokrovsky, M. B. Pykhtina, A. B. Beklemishev, D. V.

- Korchagina, K. P. Volcho, N. F. Salakhutdinov, *Med. Chem.* **2015**, *11*, 629.
- [3] a) K. Y. Ponomarev, E. V. Suslov, A. L. Zakharenko, O. D. Zakharova, A. D. Rogachev, D. V. Korchagina, A. Zafar, J. Reynisson, A. A. Nefedov, K. P. Volcho, N. F. Salakhutdinov, O. I. Lavrik, *Bioorg. Chem.* **2018**, *76*, 392; b) A. A. Chepanova, E. S. Mozhaitsev, A. A. Munkuev, E. V. Suslov, D. V. Korchagina, O. D. Zakharova, A. L. Zakharenko, J. Patel, D. M. Ayine-Tora, J. Reynisson, I. K. H. Leung, K. P. Volcho, N. F. Salakhutdinov, O. I. Lavrik, *Appl. Sci.* **2019**, *9*, 2767.
- [4] O. Concepción, J. Belmar, A. F. de la Torre, F. M. Muñiz, M. W. Pertino, B. Alarcón, V. Ormazabal, E. Nova-Lamperti, F. A. Zúñiga, C. A. Jiménez, *Molecules* **2020**, *25*, 1911.
- [5] E. V. Suslov, E. S. Mozhaitsev, D. V. Korchagina, N. I. Bormotov, O. I. Yarovaya, K. P. Volcho, O. A. Serova, A. P. Agafonov, R. A. Maksyutov, L. N. Shishkina, N. F. Salakhutdinov, *RSC Med. Chem.* **2020**, *11*, 1185.
- [6] E. Suslov, V. V. Zarubaev, A. V. Slita, K. Ponomarev, D. Korchagina, D. M. Ayine-Tora, J. Reynisson, K. Volcho, N. Salakhutdinov, *Bioorg. Med. Chem. Lett.* **2017**, *27*, 4531.
- [7] I. Philipova, V. Valcheva, R. Mihaylova, M. Mateeva, I. Doytchinova, G. Stavrakov, *Chem. Biol. Drug Des.* **2018**, *91*, 763.
- [8] a) D. S. Melo, S. S. Pereira-Junior, E. N. Dos Santos, *Appl. Catal. A* **2012**, *411*, 70; b) A. de Oliveira Dias, M. G. P. Gutiérrez, J. A. A. Villarreal, R. L. L. Carmo, K. C. B. Oliveira, A. G. Santos, E. N. dos Santos, E. V. Gusevskaya, *Appl. Catal. A* **2019**, *574*, 97; c) T. A. Faßbach, T. Gaide, M. Terhorst, A. Behr, A. J. Vorholt, *ChemCatChem* **2017**, *9*, 1359.
- [9] a) B. Zimmermann, J. Herwig, M. Beller, *Angew. Chem. Int. Ed.* **1999**, *38*, 2372; b) S. Hanna, J. C. Holder, J. F. Hartwig, *Angew. Chem. Int. Ed.* **2019**, *58*, 3368.
- [10] A. Serrano-Maldonado, T. Dang-Bao, I. Favier, I. Guerrero-Rios, D. Pla, M. Gomez, *Chem. Eur. J.* **2020**, *26*, 12553.
- [11] a) D. S. Tan, *Nat. Chem. Biol.* **2005**, *1*, 74; b) D. Pla, D. S. Tan, D. Y. Gin, *Chem. Sci.* **2014**, *5*, 2407; c) M. Camats, I. Favier, S. Mallet-Ladeira, D. Pla, M. Gómez, *Org. Biomol. Chem.* **2022**, *20*, 219.
- [12] A. Pérez Alonso, D. Pham Minh, D. Pla, M. Gómez, *ChemCatChem* **2023**, *15*, e202300501.
- [13] C. A. Belmokhtar, J. Hillion, E. Ségal-Bendirdjian, *Oncogene* **2001**, *20*, 3354.
- [14] L. Duprez, E. Wirawan, T. V. Berghe, P. Vandenabeele, *Microbes Infect.* **2009**, *11*, 1050.
- [15] a) C. S. Graebin, V. L. Eifler-Lima, R. G. da Rosa, *Catal. Commun.* **2008**, *9*, 1066; b) C. L. Kranemann, P. Eilbracht, *Synthesis* **1998**, *1*, 71.
- [16] C. S. Graebin, M. d. F. Madeira, J. K. U. Yokoyama-Yasunaka, D. C. Miguel, S. R. B. Uliana, D. Benitez, H. Cerecetto, M. González, R. G. d. Rosa, V. L. Eifler-Lima, *Eur. J. Med. Chem.* **2010**, *45*, 1524.
- [17] a) A. A. Al-Gendy, F. A. Moharram, M. A. Zarka, *J. Pharmacogn. Phytochem.* **2017**, *6*, 312; b) D. I. Hamdan, A. A. Al-Gendy, A. M. El-Shazly, *J. Pharm. Sci. Res.* **2016**, *8*, 779.

Entry for the Table of Contents



In vitro antiproliferative evaluation of a series of homologated terpene amines, prepared via a highly chemo- and regioselective Rhodium-catalyzed hydroaminomethylation strategy in 50-99% yields, revealed two lead compounds showing micromolar cytotoxicity against human colorectal cancer cells (HCT-116) with distinct activity pathways, namely growth inhibition or apoptotic cell death induction.

Institute and/or researcher Twitter usernames: @LHFA_CNRS